Short Papers

Constrained Optimal Preview Control of Dual-Stage Actuators

Aurélio T. Salton, Zhiyong Chen, Jinchuan Zheng, and Minyue Fu

***Abstract*—This paper proposes constrained optimal trajectories for the preview control of dual-stage actuators (DSA). Relying on the redundancy of actuators preview control allows the primary stage to move before the transition instant, and uses the secondary stage to compensate its movements. Contrasting existing strategies that consider the secondary stage infinitely fast during preview control, this study takes into account its dynamic limitations when designing the trajectories to be followed during preactuation. It will be shown that the problem may be cast in terms of quadratic programming providing an optimal solution with respect to a quadratic criterion. Experimental results validated the proposed strategy, which is able to achieve a 30% improvement over state-of-the-art high-performance DSA controllers, while respecting the limitations of both actuators.**

***Index Terms*—Dual-stage systems, macro/micromanipulators, motion control, nonlinear feedback, preview control.**

I. Introduction

Dual-stage actuators (DSA) were conceived in the 1980s as an attempt to improve the performance of motion systems [1]. The concept is composed of two actuators working in parallel with complementary characteristics. A primary (coarse) actuator is used to provide the system with a long range while the secondary (fine) actuator improves the system dynamics and ability to reject disturbances. Due to the complementary characteristics of the individual actuators, this class of systems also received the name macro/micromanipulator [2]. In the following decade, the concept was picked up by the hard disk drive (HDD) industry leading to the flourishing of ideas regarding both the mechanical structure and the control system design [3]. So, for several dual-stage systems, the term "track seeking" is still used to mention the movement from one reference point to another, and "track following" to mention the accuracy in which a given reference is followed under the influence of disturbances. Since the latter was the primary interest of the HDD industry, works in that time focused on the problem of disturbance rejection and track following. However, the structure of DSA is also interesting to problems related to long range and high-resolution motion control, such as the nanopositioner treated in [4] and dual-stage scanners [5].

Nonlinear control strategies designed for the track seeking improvement of linear systems have been applied to DSA in recent years. Well-known examples are the so-called proximate-time optimal servomechanism (PTOS) [6] and the composite nonlinear control [7]. These controllers, however, were originally designed to single-stage systems, and then, either applied to the primary actuator, or straightforwardly extended to DSA. Due to the fact that DSA make use of redundant actuators, any given trajectory may be achieved by different input combinations. An important contribution that explores this propriety of the DSA was given in [7]: a strategy for cooperation between the actuators was created where the primary actuator is designed to overshoot a limited amount that may be compensated by the secondary actuator, thus providing a faster rise and settling time for the overall output. Soon after, a similar idea was suggested to be applied before the output transition time in what came to be known as preview control [8]: the primary actuator is allowed to move ahead of the output transition time and relies on the secondary actuator to compensate for this movement. This strategy is based on the fact that the secondary actuator is considerably faster than the primary so that movements of the latter may be considered disturbances well inside the bandwidth of the former. In practice, this assumption is not always valid and trajectory constraints must be applied to the primary actuator so that the resulting error due to the preview movement may be satisfactorily compensated by the secondary.

This paper extends our previous work on preview control, reported in [9], to the development of *feasible* trajectories to be followed during preactuation. In particular, we present a systematic procedure in order to design trajectories the primary actuator may follow such that the track seeking time is reduced without compromising track following. Furthermore, a constraint quadratic criterion will be minimized so that an optimal trajectory that prevents the saturation of the actuators may be found. The paper is organized as follows: Sections II and III describe the DSA model and the problem at hand; a numerical solution is proposed in Section IV followed by its implementation in an experimental setup, presented in Section V; finally, Section VI concludes the paper.

Manuscript received May 21, 2014; revised August 6, 2015; accepted October 22, 2015. Date of publication November 2, 2015; date of current version February 24, 2016. Recommended by Technical Editor L. Zuo. This work was supported in part by the National Natural Science Foundation of China under Grant 51328501.

A. T. Salton is with the Pontifical Catholic University of Rio Grande do Sul, Porto Alegre 90619-900, Brazil (e-mail: aurelio.salton@pucrs.br).

Z. Chen is with the University of Newcastle, Callaghan NSW 2308, Australia, and also with the State Key Laboratory of Digital Manufacturing Equipment and Technology, Huazhong University of Science and Technology, Wuhan 430074, China (e-mail: zhiyong.chen@newcastle.edu.au).

J. Zheng is with the School of Software and Electrical Engineering, Swinburne University of Technology, Hawthorn VIC 3122, Australia (e-mail: jzheng@swin.edu.au).

M. Fu is with the University of Newcastle, Callaghan NSW 2308, Australia, and also with the Department of Control Science and Engineering, Zhejiang University, Hangzhou 310058, China (e-mail: minyue.fu@newcastle.edu.au).

Color versions of one or more of the figures in this paper are available online at http://ieeexplore.ieee.org.

Digital Object Identifier 10.1109/TMECH.2015.2496343

1083-4435 © 2015 IEEE. Personal use is permitted, but republication/redistribution requires IEEE permission.
See http://www.ieee.org/publications_standards/publications/rights/index.html for more information.

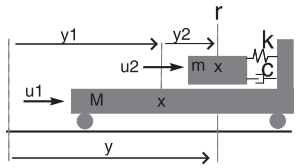

Fig. 1. Schematic representation of a typical DSA.

II. System of Interest

The system under consideration is comprised of a primary actuator modeled as a (possibly damped) double integrator, and a mass–spring–damper secondary actuator. This model is depicted in Fig. 1 and describes a general type of the DSA where a linear motor (LM) is used to drive the primary stage while a piezoelectric actuator drives the secondary stage. In the figure, r_0 is the reference being tracked and M, y_1, and u_1 (m, y_2, and u_2) are the mass, position, and input of the primary (secondary) actuator, respectively.

From Lagrangian mechanics, one may readily obtain the equations of motion of a dual-stage system

$$\ddot{y}_1 = \frac{u_1 - c_1\dot{y}_1}{M} + \frac{k_s y_2 - u_2}{M} \tag{1a}$$

$$\ddot{y}_2 = \left(\frac{1}{M} + \frac{1}{m}\right)(u_2 - c_2\dot{y}_2 - k_s y_2) - \frac{u_1}{M} \tag{1b}$$

where $f_i \in \mathbb{R}^2$ describes the external forces acting on the system

$$f_i = \text{sat}(u_i) - c_i\dot{y}_i, i = 1, 2.$$

Here, c_i are the damping coefficients of each actuator, and the saturation function $\text{sat}(u_i)$ is defined as

$$\text{sat}(u_i) = \text{sgn}(u_i)\min\{\bar{u}_i, |u_i|\}, i = 1, 2$$

for a saturation level $\bar{u}_i$.

Notice that the set of equations in (1) describes all forces acting on a typical dual-stage system, including the coupling forces between the actuators, i.e., the forces acting on the primary actuator that influence the secondary and vice versa. Such coupling may excite high frequencies and disturb the controllers, degrading the system performance. In order to avoid this interaction between the primary and secondary actuators, it is common practice to design dual-stage systems such that the masses of the actuators respect the condition $M >> m$, and that the bandwidth of the secondary actuator is higher than that of the primary actuator. By carefully picking actuators that satisfy these conditions, (1b) may be simplified to

$$\ddot{y}_2 = \frac{u_2 - k_s y_2 - c\dot{y}_2}{m} \tag{2}$$

since $1/M$ will be negligible when compared to $1/m$ and the remaining term may be considered a disturbance well inside the bandwidth of the secondary actuator. A similar discussion regarding (1a) leads to

$$\ddot{y}_1 = \frac{u_1}{M} \tag{3}$$

since $k_s y_2 - u_2 << u_1$ and c_1 is typically negligible.

Thus, the system may be modeled as two independent actuators whose only interaction comes from the system output $y = y_1 + y_2$. The aforementioned simplification of the system is a good reason to rely on piezoactuators to drive the second stage, since they match the assumptions in most situations. Therefore, a typical linear DSA may be described in its state-space form as follows:

$$\begin{aligned}
\Sigma_1 : \dot{x}_1 &= A_1 x_1 + B_1 u_1,\ x_1(0) = 0,\ |u_1| \le \bar{u}_1 \\
\Sigma_2 : \dot{x}_2 &= A_2 x_2 + B_2 u_2,\ x_2(0) = 0,\ |u_2| \le \bar{u}_2 \\
y &= y_1 + y_2 = C_1 x_1 + C_2 x_2
\end{aligned} \tag{4}$$

where $x_1 = [y_1 \ \ \dot{y}_1]^\top$ is associated with the primary actuator and $x_2 = [y_2 \ \ \dot{y}_2]^\top$ with the secondary one.

Furthermore

$$\begin{aligned}
A_1 &= \begin{bmatrix} 0 & 1 \\ 0 & 0 \end{bmatrix},\ B_1 = \begin{bmatrix} 0 \\ b_1 \end{bmatrix},\ C_1 = \begin{bmatrix} 1 & 0 \end{bmatrix} \\
A_2 &= \begin{bmatrix} 0 & 1 \\ a_1 & a_2 \end{bmatrix},\ B_2 = \begin{bmatrix} 0 \\ b_2 \end{bmatrix},\ C_2 = \begin{bmatrix} 1 & 0 \end{bmatrix}.
\end{aligned} \tag{5}$$

where $a_1 = -k_s/m$ and $a_2 = -c/m$.

III. Problem Statement

As depicted in Fig. 1, small deviations between the primary actuator and the reference are adequately compensated by the secondary actuator. This means that even if $y_1 \neq r$, it is possible that $y = r$ due to the actions of the secondary actuator. In regard to track seeking, it has been noted that the actuator redundancy may be explored by allowing the primary actuator to move ahead of time, speeding up the transition time between one reference level and another [9]. Naturally, this strategy requires the information of the future reference level and of the transition instant, i.e., the instant $t = \tau$ when the reference level will change from r_0 to r_1. Furthermore, due to the output saturation of the secondary actuator, i.e., $y_{2_{\max}} = \bar{u}_2/k_s$, the trajectories of y_1 must be constrained within the interval

$$-y_{2_{\max}} \le y_1 \le y_{2_{\max}}. \tag{6}$$

The problem of constricting the trajectories to the interval (6) was previously addressed in [9]. In this paper, we will extend those results so that the dynamic limitations of the secondary actuator—rather than only static ones—are considered in the design of the preview control trajectory.

In particular, previous works have considered the secondary actuator infinitely fast, redefining (2) to the static form $y_2 = u_2/k_s$. Then, any trajectory $z(t)$ followed by the primary actuator that satisfies $|z(t)| \le \bar{u}_2/k_s$, will be compensated by the secondary actuator, and the total output of the system will be secured at the reference. In this study, we consider a practical case with a dynamic secondary actuator. The motivation for this is the fact that a bounded input will generate bounded states, which in turn implies that the secondary actuator may not track *any* trajectory within its reach. Rather, this actuator's dynamics must be considered such that limits on $\dot{z}(t)$ and $\ddot{z}(t)$ may be imposed.

Let us define the secondary actuator tracking error as $e_t(t) := y_2(t) - z(t)$ and assume that a trajectory $z(t)$ described by

$$\kappa(z(t)) = -a_1 z(t) - a_2 \dot{z}(t) + \ddot{z}(t) \tag{7}$$

satisfies

$$|\kappa(z(t))| \leq \bar{u}_2 b_2 \tag{8}$$

for negative constants a_1 and a_2. Then, it is possible to find an input u_2 that asymptotically drives the tracking error e_t to the origin. In particular, due to the equations of system Σ_2, it is easy to verify that the choice $u_2 = \kappa(z(t))/b_2$ implies

$$\ddot{e}_t = a_1 e_t + a_2 e_t$$

which, in turn, satisfies

$$\lim_{t\to\infty} |y_2(t) - z(t)| = 0 \tag{9}$$

since $a_1,\ a_2 < 0$. Furthermore, if $y_2(0) - z(0) = 0$ and $\dot{y}_2(0) - \dot{z}(0) = 0$, then $y_2(t) = z(t)\ \ \forall t \geq 0$.

However, from the fact that the system output error is defined as

$$e(t) = y(t) - r = y_1(t) + y_2(t) - r$$

one notices that in order to achieve $e(t) = 0$ during preview control, it is necessary that $y_2(t) = r_0 - y_1(t)$, and hence, that it is the primary actuator that defines the trajectory $z(t)$ to be followed by the secondary. In other words, it is the primary actuator's trajectory that must satisfy condition (8). This is formally expressed in the next Lemma.

Lemma 1: Consider the dual-stage system described by (4), let r_0 be the reference level to be tracked during preactuation, let $y_1(t)$, $\dot{y}_1(t)$, and $\ddot{y}_1(t)$ satisfy

$$|a_1(y_1(t) - r_0) + a_2\dot{y}_1(t) - \ddot{y}_1(t)| \leq \bar{u}_2 b_2 \tag{10}$$

and let $u_2(t)$ be given by

$$u_2(t) = \frac{1}{b_2}\left(a_1(y_1 - r_0) + a_2\dot{y}_1 - \ddot{y}_1\right). \tag{11}$$

Then

$$\lim_{t\to\infty} |y_1(t) + y_2(t) - r_0| = \lim_{t\to\infty} |y(t) - r_0| = 0. \tag{12}$$

In particular, if $y(0) = r_0$ and $\dot{y}(0) = 0$, then $y(t) = r_0 \forall\, t \geq 0$.

Proof: Since $y = y_1 + y_2$ and $\dot{y} = \dot{y}_1 + \dot{y}_2$, it follows that, for the DSA in (4) with the secondary actuator under control law (11)

$$\begin{aligned}\ddot{y} &= \ddot{y}_1 + (a_1 y_2 + a_2\dot{y}_2 + b_2 u_2)\\ &= a_1(y_1 + y_2 - r_0) + a_2(\dot{y}_1 + \dot{y}_2)\\ &= a_1(y - r_0) + a_2\dot{y}\end{aligned} \tag{13}$$

which satisfies (12). Furthermore, from the assumption on the initial conditions, it is clear that $y(t) = r_0\ \ \forall t \geq 0$. □

Remark 1: Robustness may be added to controller (11) by an extra term $\gamma(e_t, \dot{e}_t) = h_1 e_t + h_2 \dot{e}_t$ with $e_t(t) = y_2(t) - (y_1(t) - r_0)$, for negative constants h_1 and h_2. The secondary actuator control law is then defined as

$$u_2(t) = \frac{1}{b_2}\left(a_1(y_1 - r_0) + a_2\dot{y}_1 - \ddot{y}_1 + \gamma(e_t)\right). \tag{14}$$

This term will compensate deviations from the desired trajectory due to initial conditions, disturbances and/or model uncertainties, but may be neglected during the computation of $\kappa(\cdot)$. This will be shown in Section V, where successful experimental results are demonstrated.

Given Lemma 1 it is now straightforward to define the problem addressed in this study: find a preview control trajectory for $y_1(t)$ that is able to both satisfy the conditions given in (10) and improve the performance of the system by being closer to and moving toward r_1 at the switching time $t = \tau$.

IV. Constrained Optimal Preview Control

The approach taken in this paper is that of framing problem stated in Section III in a quadratic programming (QP) form. In order to do so, it is first necessary to discretize the system. Henceforth, the following notation will be used to describe the primary actuator in discrete form:

$$x_{d1}(k+1) = A_d x_{d1}(k) + B_d u_1(k) \tag{15}$$

where $x_{d1}(k) \in \mathbb{R}^2$ are the discrete equivalent of the primary actuator states and $u_1(k) \in \mathbb{R}$ is its input. The matrices A_d and B_d are obtained from matrices A_1 and B_1 in (4) via some discretization method with sampling time T , e.g., Euler Forward. The solution sought is the set of discrete inputs to be applied to the primary actuator during preview control

$$\mathbf{u_1} = [\hat{u}_1(0)\ \hat{u}_1(1)\ \ldots \hat{u}_1(N)]^\top \tag{16}$$

that satisfy the discrete version of constraint (10), namely

$$[a_1\ a_2]\, x_{d1}(k) - b_1 u_1(k) \leq b_2 \bar{u}_2. \tag{17}$$

On the aforementioned, we have assumed $r_0 = 0$ and used the system equations $\ddot{y}_1(t) = b_1 u_1(t)$ in order to simplify the exposition. Also, $NT = \tau$ is the duration of preactuation, and N the so-called prediction horizon.

In order to obtain $\mathbf{u_1}$, we consider the following cost function:

$$V := \frac{1}{2}(x_{d1}(N) - x_s)^\top P (x_{d1}(N) - x_s) + \sum_{k=0}^{N-1} \Lambda_k \tag{18}$$

where

$$\Lambda_k := \frac{1}{2}\left(x_{d1}(k)^\top Q x_{d1}(k) + u_1(k)^\top R u_1(k)\right) \tag{19}$$

$P,\ Q \geq 0$, and $R > 0$ are free weight matrices and x_s represents the desired states for the primary actuator at the transition instant $t = \tau$. With this cost function and an appropriate choice of the matrices P, Q, R, and x_s, it is possible to design a trajectory that minimizes the distance $|r_1 - y_1|$ and maximizes the speed in which y_1 approaches r_1 at the final instant of the trajectory $(t = \tau)$.

Recall that the problem of minimizing the cost function (18) is equivalent to finding the vector $\mathbf{u_1}(x) \in \mathbb{R}^N$ given by

$$\mathbf{u_1} = \arg\min_{L\mathbf{u_1} \leq Z} \frac{1}{2}\mathbf{u_1}^\top \mathcal{H}\mathbf{u_1} + \mathbf{u_1}^\top F(x - x_s). \tag{20}$$

where $\mathcal{H} = \Gamma^\top \mathbf{Q}\Gamma + \mathbf{R}$ is the so-called *Hessian* of QP and L and Z describe the constrains that must be respected [10]. The

matrices may be defined as follows:

$$F = \Gamma^\top \mathbf{Q}\Omega, \Gamma := \begin{bmatrix} B_d & 0 & \dots & 0 & 0 \\ A_d B_d & B_d & \dots & 0 & 0 \\ \vdots & \vdots & \ddots & \vdots & \vdots \\ A_d^{N-1} B_d & A_d^{N-2} B_d & \dots & \ddots & B_d \end{bmatrix} \tag{21}$$

with

$$\begin{aligned} \mathbf{Q} &:= \text{diag}\{C^\top QC, \dots, C^\top QC, P\} \\ \mathbf{R} &:= \text{diag}\{R, \dots, R\} \\ \Omega &:= \begin{bmatrix} A_d & A_d^2 & \dots & A_d^N \end{bmatrix}^\top. \end{aligned} \tag{22}$$

The necessary constraints on the input $|u_1| \leq \bar{u}_1$ and on the trajectory of the primary actuator as given in (10) are readily included in this formulation through matrices L and Z. Thus, trajectories for the primary actuator during preview control that are feasible in the sense of (17) and optimal in the sense of (18) may be computed according to the following theorem.

Theorem 1: Consider system (4) with the secondary actuator control law u_2 as in (11). Let the primary actuator follow a trajectory given by (20) through (22) during preactuation, and define the matrices L and Z as follows:

$$L = \begin{bmatrix} I_N \\ \Psi \\ -I_N \\ -\Psi \end{bmatrix}, \; Z = \begin{bmatrix} \mathbf{u}^1_{\max} \\ \tilde{Z} \\ \mathbf{u}^1_{\max} \\ -\tilde{Z} \end{bmatrix} \tag{23}$$

where I_N is the $N \times N$ identity matrix

$$\Psi = \begin{bmatrix} \psi & 0 & 0 & \dots & 0 \\ 0 & \psi & 0 & \dots & 0 \\ 0 & 0 & \psi & \dots & 0 \\ \vdots & \vdots & \vdots & \ddots & \vdots \\ 0 & 0 & 0 & \dots & \psi \end{bmatrix} \Gamma - b_1 \begin{bmatrix} 0 & 1 & 0 & \dots & 0 \\ 0 & 0 & 1 & \dots & 0 \\ \vdots & \vdots & \vdots & \ddots & \vdots \\ 0 & 0 & 0 & \dots & 1 \\ 0 & 0 & 0 & \dots & 0 \end{bmatrix} \tag{24}$$

and

$$\begin{aligned} \tilde{Z} &:= -\psi \Omega x_{d1}(0) + b_2 \mathbf{u}^2_{\max} \\ \psi &:= \begin{bmatrix} a_1 & a_2 \end{bmatrix} \\ \mathbf{u}^i_{\max} &:= \begin{bmatrix} \bar{u}_i & \dots & \bar{u}_i \end{bmatrix}^\top \end{aligned} \tag{25}$$

for $i = 1, 2$. Then, given $y(0) = r_0$ and $\dot{y}(0) = 0$

$$y(k) = r_0, \; 0 \leq k \leq N.$$

That is, the tracking of r_0 is achieved during preactuation.

Proof: From Lemma 1, it follows that if inequality (17) is satisfied, then $y(k) = r_0$ during preactuation. In order to satisfy (17) note that the multiplication of any row of Ψ by $\mathbf{u_1}$ will result in

$$\begin{aligned} \psi B_d \hat{u}_1(k) - b_1 \hat{u}_1(k+1) &\leq -A_d^k x_{d1}(0) + b_2 \bar{u}_2 \\ \psi x_{d1}(k+1) - b_1 \hat{u}_1(k+1) &\leq b_2 \bar{u}_2 \end{aligned} \tag{26}$$

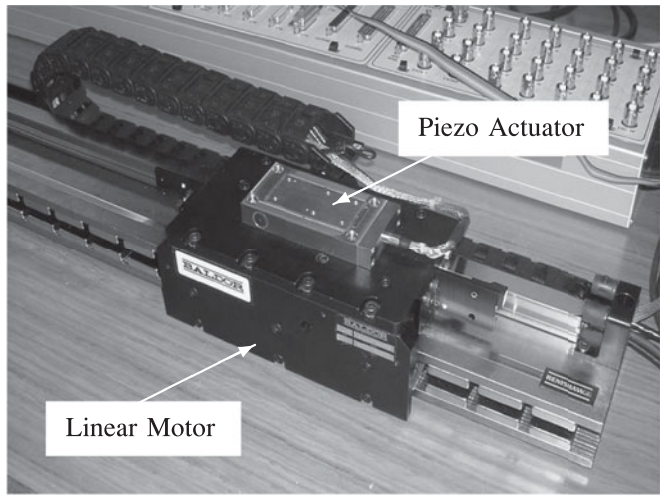

Fig. 2. Picture of the experimental setup comprised by an LM and a piezoelectric actuator.

for $k = 0 \dots N-1$, satisfying condition (17) for all points in the trajectory. Furthermore, the constraints on the control effort are obviously satisfied from $I_N \mathbf{u_1} \leq \mathbf{u}^1_{\max}$, resulting in a feasible trajectory both for the primary and secondary actuator. □

Remark 2: From the solution (16), a reference trajectory $\hat{x}_{d1} = [\hat{y}_1 \; \dot{\hat{y}}_1]^\top$ may be computed and tracked via some classical controller such as state feedback

$$u_1(k) = \hat{u}_1(k) + W(x_{d1}(k) - \hat{x}_{d1}(k)). \tag{27}$$

The combined use of (16) with a PD controller adds some robustness to the system since small deviations from the desired trajectory may be compensated. It turns out that the solution provided by quadratic programming generated a rather interesting and unexpected trajectory described in what follows.

V. Implementation

The DSA used to validate the proposed design is depicted in Fig. 2 and comprises a LM as the first stage and a piezoelectric actuator (piezo) as the second one. While the piezo actuator's range is limited in ± 15 μm and has an integrated capacitive position sensor with 2-nm resolution, the LM has a traveling range of 0.5 m and a 1-μm resolution glass scale encoder. Since the capacitive sensor is used to measure the incremental displacement provided by the piezo in relation to the LM, the system output is limited by the resolution of the LM encoder. While the primary actuator is dominated by the dynamics of a rigid body and well described by a double integrator, the piezo actuator is of high stiffness and follows a flat gain in low frequencies. Furthermore, the interaction between the actuators is minimal, making the testbed well suited for the application of the developed controller. The DSA setup is fully described by (4) with the following parameters:

$$\begin{aligned} a_1 &= -10^6, \; b_1 = 1.7 \times 10^7, \; \bar{u}_1 = 1 \\ a_2 &= -1810, \; \; b_2 = 3 \times 10^6, \; \; \bar{u}_2 = 5. \end{aligned} \tag{28}$$

For further details, please refer to [7] where this system identification procedure is given.

A. Secondary Actuator Control Law

Several advanced techniques relating to piezoeletric actuators could be employed to the control of the secondary actuator [11], [12]. However, for the purpose of this study, the secondary actuator controller will be given by the simple expression in (14) and will be maintained both during and after preactuation. The applied control law becomes

$$u_2 = \frac{1}{b_2}((y_1 - r_0)a_1 + \dot{y}_1 a_2 - \ddot{y}_1 + \gamma(\cdot))$$

$$\gamma(x_1, x_2, r) = H \begin{bmatrix} y_2 - (y_1 - r) \\ \dot{y}_2 - \dot{y}_1 \end{bmatrix} \tag{29}$$

with $H = [h_1 \;\; h_2]$ a linear gain that may be designed via classical methods of control systems' theory. In this case

$$H = [83.85 \;\; 0.036] \times 10^{-2}. \tag{30}$$

B. Primary Actuator Control Law

The primary actuator will be subject to two different controllers, one during the preview control interval, and another one after it. For $0 < t \leq \tau$, the controller calculated in Section IV is used. This is now a "responsible" form of preview control that achieves a faster performance without compromising the tracking of r_0. The optimization problem is solved with $T = 0.1$ ms, $N = 200$, $R = 1.5 \times 10^4$, $Q = 10^{-3}$ and

$$P = \begin{bmatrix} 10^3 & 0 \\ 0 & 10^{-1} \end{bmatrix}.$$

When $t > \tau$, the preview control is over and the system output y must now track r_1 instead r_0. While the secondary actuator controller may remain unchanged, the primary control law must switch to some form of fast tracking control. There are several forms of advanced controllers for fast tracking servomechanisms [13], but, since the primary actuator controller outside the preview control interval is not the main contribution in this study, the traditional PTOS will be used. This strategy is an improved approximation of the time-optimal control in the sense that it does not suffer from chattering. The PTOS control law is given by

$$u_1(t) = k_2(-f_{\text{ptos}}(e_1) - \dot{y}_1)$$

with $e_1 := y_1 - r$ and

$$f_{\text{ptos}}(e_1) = \begin{cases} (k_1/k_2)e_1, & \text{for } |e_1| \leq y_l \\ \text{sgn}(e)(\sqrt{2b_1\alpha\bar{u}_1|e_1|} - \bar{u}_1/k_2), & \text{for } |e_1| > y_l. \end{cases}$$

A stability condition requires that $0 < \alpha < 1$, and the following constraints guarantee the continuity of the controller:

$$y_l = \frac{\bar{u}_1}{k_1}, \quad k_2 = \sqrt{\frac{2k_1}{b_1\alpha}}.$$

This controller has several interesting properties whose detailed descriptions are outside the scope of this paper. Here, its ability to overshoot a controlled amount is explored. As proposed in [7], one may allow this controller to overshoot without surpassing the limitation of the secondary actuator. Since this overshoot is compensated by the second stage, the total output

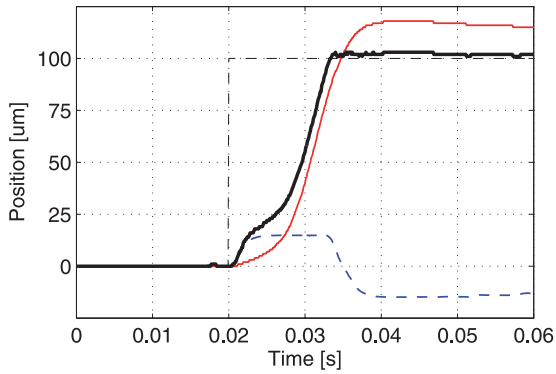

Fig. 3. DSA hig-performance control without the use of preview control. The primary actuator (thin line) overshoots a desired amount, the secondary actuator (dashed line) compensates for the overshoot achieving a settling time of 13 ms (thick black line).

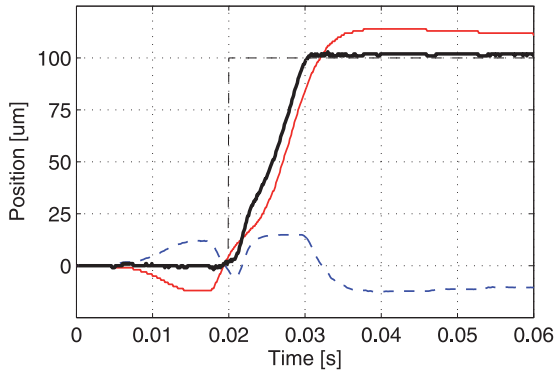

Fig. 4. Proposed controller with the preview control strategy. The settling time of 10 ms indicates a 30% improvement due to preview control.

rise time is faster. This will be clear during the discussion on the obtained results. The controller is tuned as follows:

$$\alpha = 0.7, \;\; k_1 = 2.09, \;\; k_2 = 0.019. \tag{31}$$

Finally, since no velocity sensors were available in the implementation setup, state observers were used to reconstruct the unmeasured states, i.e., the actuators' velocities.

C. Results

Figs. 3 and 4 compare the same DSA controller with and without the aid of preview control. In both figures, the primary actuator is depicted as the thin line, the secondary one as the dashed line, and the total output as the thick black line. Results given by the controller that does not make use of preview control are shown in Fig. 3. This figure shows the advantage of allowing the primary actuator to overshoot, i.e., as soon as this actuator is sufficiently close to r_1, the secondary reaches the reference and achieves $y = r_1$ within a small tolerance (in this case ± 2 μm). The resulting settling time is 13 ms and considerably faster than what the system would achieve with the primary actuator alone.

The plot in Fig. 4 shows the preview control strategy working with a trajectory designed according to Theorem 1. Note that the primary actuator moves away from the future reference r_1 in the first moments of preactuation so that it may accelerate toward r_1 before the switching instant $t = \tau = 0.02$ s arises. The

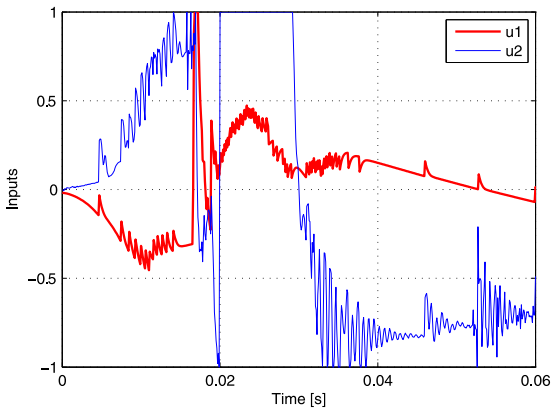

Fig. 5. Input responses for a reference step of 100 μm. During preview control, the actuators' saturation levels are respected and track following is not compromised.

resulting improvement is of about 30% since the settling time with preview control is 10 ms. It is also important to emphasize that during preactuation the tracking of r_0 is not compromised and both input signals are within the limits given by saturation, as depicted in Fig. 5.

D. Discussion

The faster dynamics of the second stage is well exemplified in Fig. 3 (dashed line), where the secondary actuator rushes toward the new reference level r_1 only to saturate immediately after. It stays saturated till the primary actuator (thin line) is sufficiently close to the reference, showing that the system is severely limited by the dynamics of the slow actuator whenever the fast actuator is saturated. In other words, whenever the second stage is saturated, the system's response is only as fast as the first stage. Fig. 4, on the other hand, uses preview control to improve the performance of the primary actuator, reducing the time it takes to reach the reference after preactuation. As a result, the system dynamics is dominated by the secondary actuator because it leaves its saturated condition sooner. Since this actuator is considerably faster than the primary, a remarkable performance improvement is achieved.

The success of this strategy, however, is entirely dependent on the system's ability to track r_0 during preactuation, inasmuch as any movement away from this reference level could compromise the control application. Therefore, not only the trajectory followed by the primary actuator must be in range of the secondary during this period, it must also respect the dynamic limitations of the fast actuator. The computation of such *safe* trajectory, depicted in Fig. 4, was the objective of this paper. Furthermore, Fig. 5 shows that both actuators respect their input saturation levels during preview control, a necessary condition in order to achieve $y = r_0$. After the transition instant, however, when the output is being transferred from r_0 to r_1, the actuators are free to saturate so a fast response is achieved.

Remark 3: Since the secondary actuator has a considerably faster dynamics than that of the primary, it perceives the trajectory error as a series of steps caused by the sensor quantization of the LM (recall that u_2 is a function of $r - y_1$). This causes an apparent chattering in the input of the fast actuator, as shown in Fig. 5 . However, if not for the quantization of y_1, the chattering would not be present.

VI. Conclusion

This paper has proposed constrained optimal trajectories for the preview control of DSA. In particular, the limitations of the secondary actuator were carefully taken into account when designing the trajectories to be followed during preview control. Thus, the proposed approach provides guarantees that the output will remain at the reference prior to the transition instant. In order to achieve this *safe* form of preview control, not only static but also dynamic constraints have been considered. The problem was cast in terms of quadratic programming so that a quadratic criterion could be minimized, providing an optimal solution. Experimental results validated the proposed strategy, which was able to achieve a 30% improvement over state-of-the-art high-performance controllers for the DSA.

References

[1] M. Kanai, N. Takeuchi, and H. Kinoshita, "An elastic fine positioning mechanism applied to contactless x–y table," *Bull. Japan Soc. Prec. Eng.*, vol. 17, no. 4, pp. 265–266, 1983.

[2] A. Sharon and D. Hardt, "Enhancement of robot accuracy using endpoint feedback and a macro-micro manipulator system," in *Proc. Amer. Control Conf.*, 1984, pp. 1836–1845.

[3] J.-Y. Yen, K. Hallamasek, and R. Horowitz, "Track-following controller design for a compound disk drive actuator," *J. Dyn. Syst., Meas. Control*, vol. 112, no. 3, pp. 391–402, 1990.

[4] H.-Y. Wang, K.-C. Fan, J.-K. Ye, and C.-H. Lin, "A long-stroke nanopositioning control system of the coplanar stage," *IEEE/ASME Trans. Mechatronics*, vol. 19, no. 1, pp. 348–356, Feb 2014.

[5] T. Tuma, W. Haeberle, H. Rothuizen, J. Lygeros, A. Pantazi, and A. Sebastian, "A high-speed electromagnetically-actuated scanner for dual-stage nanopositioning," in *Proc. IFAC Symp. Mechatronic Syst.*, 2013, pp. 125–130.

[6] M. Workman, R. Kosut, and G. Franklin, "Adaptive proximate time-optimal servomechanisms: Discrete-time case," in *Proc. IEEE 26th Conf. Decision Control*, 1987, vol. 26, pp. 1548–1553.

[7] J. Zheng and M. Fu, "Nonlinear feedback control of a dual-stage actuator system for reduced settling time," *IEEE Trans. Control Syst. Technol.*, vol. 16, no. 4, pp. 717–725, Jul. 2008.

[8] D. Iamratanakul, B. Jordan, K. K. Leang, and S. Devasia, "Optimal output transitions for dual-stage systems," *IEEE Trans. Control Syst. Technol.*, vol. 16, no. 5, pp. 869–881, Sep. 2008.

[9] A. T. Salton, Z. Chen, J. Zheng, and M. Fu, "Preview control of dual-stage actuator systems for superfast transition time," *IEEE/ASME Trans. Mechatronics*, vol. 16, no. 4, pp. 758–763, Aug. 2011.

[10] G. C. Goodwin and J. A. De Doná, *Constrained Control and Estimation: An Optimisation Approach*. New York, NY, USA: Springer, 2005.

[11] G.-Y. Gu, L.-M. Zhu, C.-Y. Su, and H. Ding, "Motion control of piezoelectric positioning stages: Modeling, controller design, and experimental evaluation," *IEEE/ASME Trans. Mechatronics*, vol. 18, no. 5, pp. 1459–1471, Oct. 2013.

[12] J. Peng and X. Chen, "Integrated PID-based sliding mode state estimation and control for piezoelectric actuators," *IEEE/ASME Trans. Mechatronics*, vol. 19, no. 1, pp. 88–99, Feb. 2014.

[13] A. T. Salton, Z. Chen, and M. Fu, "Improved control design methods for proximate time-optimal servomechanisms," *IEEE/ASME Trans. Mechatronics*, vol. 17, no. 6, pp. 1049–1058, Dec. 2012.